# Transplacental innate immune training via maternal microbial exposure: the XBP1-ERN1 axis in programming dendritic cell precursors

**Authors:** Kyle T. Mincham[1], Anya C. Jones[1], Marie Bodinier[2], Naomi M. Scott[1], Jean-Francois Lauzon-Joset[1,3], Philip A. Stumbles[1,4], Anthony Bosco[1], Patrick G. Holt[1,5†], Deborah H. Strickland[1†*]

**Affiliations:**

[1]Telethon Kids Institute, University of Western Australia, Nedlands, Western Australia, Australia.

[2]INRA Pays de la Loire, UR 1268 Biopolymers Interactions Assemblies (BIA) Nantes, Nantes, France.

[3]Centre de recherche de l'Institut de Cardiologie et de Pneumologie de Québec, Université Laval, Québec, Canada.

[4]College of Science, Health, Engineering and Education, Murdoch University, Perth, Western Australia, Australia.

[5]Child Health Research Centre, The University of Queensland, Brisbane, Australia.

[†]Joint senior authors.

[*]Corresponding author. Email: Deb.Strickland@telethonkids.org.au Ph: +61 8 6319 1528 Address: Northern Entrance, Perth Children's Hospital, 15 Hospital Avenue, Nedlands, Western Australia, 6009.

**Conflict of interest statement:** The authors have declared that no conflict of interest exists.

**Abstract**

We recently reported that the offspring of mice treated during pregnancy with the microbial-derived immunomodulator OM-85 manifest striking resistance postnatally to allergic airways inflammation, and localised the potential treatment target to the fetal cDC progenitor compartment which expands to increase the pool of precursors available at birth, enabling accelerated postnatal seeding of the lung mucosal cDC network required for establishment of immunological homeostasis in the airways. Here, we profile maternal OM-85 treatment-associated transcriptomic signatures in fetal bone marrow, and identify a series of immunometabolic pathways which provide essential metabolites for accelerated myelopoiesis, that are hallmarks of classical "immune training". In addition, the cDC progenitor compartment displayed treatment-associated activation of the XBP1-ERN1 signalling axis which has previously been shown to be essential for tissue survival of cDC, particularly within the lung microenvironment. Our forerunner studies indicate uniquely rapid turnover of airway mucosal cDCs at baseline, with further large-scale upregulation of population dynamics during aeroallergen and/or pathogen challenge. XBP1-ERN1 signalling plays a key role in mitigation of ER stress-associated toxicity which frequently accompanies DC hyper-activation during intense immunoinflammatory responses, and we suggest that enhanced capacity for XBP1-ERN1-dependent cDC survival within the airway mucosal tissue microenvironment may be a crucial element of the OM-85-mediated transplacental "innate immune training" process which results in enhanced resistance to airway inflammatory disease during the high-risk early postnatal period.

49 **Introduction**

50 The neonatal period represents a time of high risk for infection-related morbidity/mortality
51 resulting from the combined effects of maturational deficiencies in both anti-microbial
52 defense mechanisms that mediate pathogen recognition and elimination, and in the
53 accompanying regulatory mechanisms required for calibration of these responses to minimise
54 inflammatory damage to host tissues[1, 2]. With respect specifically to the lung tissue
55 microenvironment, a crucial factor governing the kinetics of postnatal acquisition of immune
56 competence is the rate of development of the airway mucosal cDC network which controls
57 local immune surveillance[3, 4].

58

59 In addition to increased susceptibility to infectious diseases, the seeds for development of a
60 range of non-communicable diseases exemplified by asthma and aero-allergies are also
61 frequently sewn during this early postnatal window period[5], suggesting that maturational
62 deficiencies in immune function(s) may also be risk factors in this context. In this regard,
63 maternal immune perturbations have been acknowledged to significantly influence fetal
64 immune development, but the underlying mechanisms remain poorly characterised[6].
65 Emerging epidemiological data from studies on traditional farming families in Europe and USA
66 suggesting that benign environmental microbial exposures of mothers during pregnancy can
67 promote prenatal immune maturation within their offspring, leading to reduced susceptibility
68 to postnatal development of respiratory inflammatory diseases[7, 8], have stimulated wide-
69 spread interest in this issue. This capacity for microbial exposures to modulate immune
70 development is consistent with the paradigm of "immune training", whereby exposure to
71 certain classes of microbial stimuli can alter the long-term functional state of innate immune
72 cells, occurring at the progenitor level in the bone marrow (BM)[9-11], leading to optimised

73 peripheral immune responsiveness to other unrelated microorganisms[12]. With this in mind,
74 there is growing interest in the concept that immune training can be therapeutically
75 harnessed[13], particularly during prenatal development, to enhance immunocompetence
76 within the offspring[14].
77
78 We recently reported that oral treatment of pregnant mice with the microbial-derived
79 immunomodulatory agent OM-85 reduces susceptibility of their offspring to the development
80 of Th2-driven allergic airways inflammation, and identified myeloid progenitors in the
81 offspring BM (which supply precursor DC to eventually populate mucosal DC networks) as a
82 major target for maternal treatment effects[15]. In the study presented here, we employed
83 transcriptomic profiling to characterise gene networks activated in fetal BM (fBM) as a result
84 of maternal OM-85 treatment, and identify the principal treatment targets as
85 immunometabolic pathways supplying cellular cholesterol essential for rapid expansion of
86 myeloid precursor compartments, and which have previously been recognised as hallmarks
87 of classical immune training-associated gene signatures. We additionally identify a specific
88 pathway in the cDC precursor compartment which has previously been associated with
89 survival-under-stress, especially within the lung mucosal microenvironment.
90
91 **Results**
92 To elucidate the mechanisms-of-action of maternal OM-85 treatment, we examined the *in*
93 *utero* fetal response at gestation day 18.5 (Figure 1A), 2 days prior to expected natural term
94 delivery.
95

96 ***Maternal OM-85 treatment selectively accelerates functional maturation of cDCs in fetal***
97 ***bone marrow***
98 Phenotypic analysis of the fBM myeloid compartment using multicolour flow cytometry
99 revealed significant expansion of the total dendritic cell (DC) pool in fetuses from OM-85
100 treated mothers as compared to equivalent fetal samples from untreated mothers (Figure
101 1B). Further characterisation of the BM DC response demonstrated that this increase was
102 restricted to the conventional DC (cDC) subset as previously described[15], with no parallel
103 changes observed in plasmacytoid DC (pDC) (Figure 1B). These cDC-specific changes in fBM
104 mirror our recent observations of increased cDC yields from BM cultures and peripheral lung
105 from the offspring of OM-85-treated mothers in the early postnatal period[15]. We next turned
106 our attention to fetal DC maturation state as determined by surface I-A/I-E expression. As
107 shown in Figure 1C, maternal OM-85 treatment for the last half of gestation enhanced I-A/I-
108 E expression on cDC in fBM when compared to fBM cDC from untreated mothers. Collectively,
109 these observations suggest that transplacental signals generated at the feto-maternal
110 interface following OM-85 treatment during pregnancy can "train" the developing fetal
111 immune system via accelerating the development of functional competence within the fBM
112 cDC compartment.
113
114 ***Expansion of fetal bone marrow myeloid progenitor subsets following maternal OM-85***
115 ***treatment***
116 Previous studies from our laboratory have additionally identified postnatal expansion of BM
117 myeloid progenitor (MP) cell populations as an effect of maternal treatment with OM-85
118 during pregnancy[15]. These findings mirror that of recent studies which identified modulation
119 of BM MP as an important component of conventional immune training mediated by both β-

120 glucan-[10] and Bacillus Calmette-Guérin (BCG)[11]. Based on these findings, we hypothesised
121 that the enhanced cDC population within fBM following maternal OM-85 treatment would
122 also be accompanied by concomitant upregulation of upstream MP subsets. Flow cytometric
123 analysis of fBM (Figure 2A) $Lin^{-}IL\text{-}7R\alpha^{-}c\text{-}Kit^{+}Sca\text{-}1^{-}$ MP (Figure 2B), $Lin^{-}IL\text{-}7R\alpha^{-}c\text{-}Kit^{+}Sca\text{-}1^{-}$
124 $CD16/32^{hi}CD34^{+}$ granulocyte-macrophage progenitor (GMP; Figure 2C) and $Lin^{-}IL\text{-}7R\alpha^{-}c\text{-}$
125 $Kit^{+}Sca\text{-}1^{-}CD16/32^{hi}CD34^{+}CX3CR1^{+}Flt\text{-}3^{+}$ macrophage-dendritic cell progenitor (MDP; Figure
126 2D) populations demonstrated a total increase in all 3 progenitor subsets within the BM
127 compartment following maternal OM-85 treatment, when compared to fBM from untreated
128 mothers. Consistent with the findings in Figure 1B and C, these data provide further evidence
129 that maternal OM-85 treatment selectively modulates the offspring BM myeloid lineage *in*
130 *utero*, beginning at the early-stage myeloid progenitor level through to the terminal cDC
131 populations which are responsible for seeding peripheral tissues during early postnatal life to
132 provide local DC-mediated immune surveillance.
133
134 ***Maternal OM-85 treatment activates key regulators of the UPR pathway in fetal bone***
135 ***marrow***
136 To gain further insight into the molecular mechanisms underpinning the maternal OM-85-
137 treatment effects, we employed transcriptomic profiling of fBM cells. Comparison of the
138 transcriptomic profiles in the treated versus untreated groups indicated that maternal OM-
139 85 treatment resulted in 152 differentially expressed genes (DEG) in fBM (119 upregulated,
140 33 downregulated; Figure 3A, Supplementary Table 1). We then interrogated the DEG for
141 enrichment of biological pathways employing *InnateDB*[16], focusing on the upregulated DEG
142 response given the limited number of downregulated DEG identified. In fBM, upregulated
143 DEG were enriched for genes involved in multiple aspects of protein metabolism, the

144 endoplasmic reticulum (ER) stress response, the unfolded protein response (UPR), cholesterol
145 biosynthesis and lipid metabolism (Supplementary Table 2).
146
147 Upstream regulator analysis was then performed to identify putative molecular drivers of all
148 observed DEG. The data revealed X-box binding protein 1 (XBP1), a transcription factor central
149 to the UPR[17] and crucial in the development, survival and function of multiple cell types
150 including plasma cells[18], eosinophils[19], natural killer (NK) cells[20], T-cell subsets[21] and DCs[22, 23],
151 as the most strongly activated molecular driver within fBM associated with maternal OM-85
152 treatment effects (*P*-value = $3.81 \times 10^{-17}$, Z-score = 4.427, Figure 3B; Supplementary Table 3),
153 and consistent with this, its downstream target, the canonical UPR sensor Activating
154 Transcription Factor 6 beta (ATF6$\beta$)[24, 25] was upregulated (Supplementary Table 1 and 3).
155 Additionally, Endoplasmic Reticulum To Nucleus Signalling 1 (ERN1) was identified as an
156 activated driver gene within the fBM following maternal OM-85 treatment (*P*-value = $3.32 \times 10^{-}$
157 $^{6}$, Z-score = 2.156; Figure 3B; Supplementary Table 3). Identification of ERN1 is crucial given
158 that during the ER stress response, this gene encodes the ER stress sensor protein inositol-
159 requiring enzyme 1 (IRE1$\alpha$), responsible for the unconventional cleavage of a 26 nucleotide
160 fragment from *Xbp1* mRNA, resulting in the generation of the active spliced variant of XBP1
161 (XBP1s) and enabling it to function as a potent transcription factor within the UPR signalling
162 pathway[25]. Collectively, these findings suggest that activation of the UPR pathway may be a
163 central component of the immune training mechanism induced in fBM as a result of maternal
164 OM-85 treatment. In addition to UPR pathway drivers, maternal OM-85 treatment also
165 resulted in the upstream activation of multiple drivers central to immunometabolic pathways
166 involved in cellular cholesterol homeostasis, including Sterol Regulatory Element Binding
167 Transcription Factor 1 (SREBF1; *P*-value = $1.95 \times 10^{-6}$, Z-score = 3.056) and 2 (SREBF2; *P*-value

168 = $2.95 \times 10^{-9}$, Z-score = 2.745) and Sterol Regulatory Element Binding Protein Cleavage-
169 Activating Protein (SCAP; *P*-value = $1.52 \times 10^{-10}$, Z-score = 2.949; Figure 3B; Supplementary
170 Table 3). This was associated with upregulation of their downstream target Low-Density
171 Lipoprotein Receptor (LDLR; Supplementary Table 1 and 3), while Insulin Inducible Gene 1
172 (INSIG1) was inhibited in fBM following maternal OM-85 treatment (*P*-value = $5.81 \times 10^{-8}$, Z-
173 score = -2.931; Figure 3B; Supplementary Table 3).
174
175 Additional candidate drivers in fBM following maternal OM-85 treatment included CD38, IL5,
176 and an array of microRNAs (miR) (Figure 3B; Supplementary Table 3) recognised principally in
177 the context of cancer-associated functions[26-28]. Of note, miR-149-3p (strongly downregulated
178 in Figure 3B) has been shown to negatively regulate Toll-like receptor (TLR) 4 expression in
179 murine monocytic cells *in vitro*[29] and it is possible that other miRs may have similar (but as
180 yet undefined) innate immune regulatory functions[30]. The relevance of finding TLR4
181 upregulation in BM-derived myeloid cells in this model merits further investigation. Likewise,
182 the identification of the T-cell activation-associated markers CD38 and IL-5 suggests possible
183 contributions from activated T-cells, and these possibilities will also be addressed in follow up
184 studies.
185
186 ***Upregulation of XBP1s expression is restricted to fetal bone marrow cDC precursors***
187 ***following maternal OM-85 treatment***
188 Finally, to obtain evidence confirming that the activated form of XBP1 was upregulated, we
189 measured expression of the active spliced variant of XBP1 (XBP1s) at the protein level within
190 fBM. Using multicolour flow cytometry, we identified significant upregulation of fBM
191 $CD11b^{+}CD11c^{+}$ pre-cDCs expressing intracellular XBP1s following maternal OM-85 treatment

192 (Figure 4A, B). While intracellular XBP1s expression was additionally localised within fetal
193 $CD19^{+}B220^{+}$ B cells, $NKp46^{+}CD11b^{+}B220^{+}CD11c^{lo}$ NK cells and $CD3^{+}$ T-cells (Supplementary
194 Figure 1), as previously described in the literature[18, 20, 21, 31], maternal OM-85 treatment had
195 no impact on XBP1s expression levels in these cell types.
196
197 **Discussion**
198 In this study, we have characterised the response of the fBM myeloid cell compartment to
199 maternal treatment with the microbial-derived innate immune modulator OM-85 during
200 pregnancy. We demonstrate that, consistent with our previous reports in 6-week-old
201 offspring[15], maternal OM-85 treatment expanded the baseline pool of GMP and MDP in fBM.
202 Furthermore, we show for the first time the maternal OM-85-induced modulation of
203 metabolic pathways within fBM responsible for cellular cholesterol homeostasis, with specific
204 activation of SREBF1, SREBF2, SCAP and LDLR. In this regard, SREBF1 and SREBF2 are
205 responsible for encoding sterol regulatory element binding proteins (SREBP) which play a
206 central role in cellular metabolism by controlling the synthesis of cholesterol and other
207 membrane lipids in the Golgi of mammalian cells, with SREBP2 (encoded by SREBF2) regarded
208 as the "master regulator" of cellular cholesterol biosynthesis[32]. Furthermore, SCAP is central
209 to this process by acting as a protein chaperone, mediating the transport of SREBP from the
210 ER to the Golgi to promote cholesterol biosynthesis[32]. In parallel with this metabolic pathway,
211 LDLR regulates cellular uptake of low-density lipoprotein (LDL), the upregulation of which
212 increases downstream cholesterol accumulation within the cell and is required for the
213 proliferation of hematopoietic stem and progenitor cells[33]. It is now recognised that
214 myelopoiesis within the BM is heavily reliant upon an increased demand for cellular
215 cholesterol and enhanced cholesterol biosynthesis[34-36], and we therefore postulate that

216 upregulation of this immunometabolic pathway following maternal OM-85 treatment is in-
217 part responsible for the expansion of MP, GMP and MDP observed within fBM. Further
218 reinforcing the importance of enhanced cholesterol biosynthesis, INSIG1, an ER membrane
219 protein that prevents trafficking of SCAP/SREBP complexes to the Golgi and thereby restrains
220 cholesterol biosynthesis[37], was inhibited in fBM following maternal OM-85 treatment.
221 Together, these findings parallel previous studies demonstrating that enhanced cellular
222 cholesterol biosynthesis and resultant expansion of BM MP is a hallmark of classical β-glucan-
223 mediated central immune training[10]. We further demonstrate that transplacental
224 mechanisms promoting maternal OM-85-induced immune training within fBM involve a
225 dynamic process comprising upregulation of immunometabolic pathways that provide key
226 rate-limiting metabolites required for myelopoiesis and subsequent expansion of MP, GMP
227 and MDP, and concomitant inhibition of negative feedback loops responsible for arresting
228 cholesterol biosynthesis.
229
230 Downstream of the fBM progenitor response, maternal OM-85 treatment selectively
231 amplified the overall abundance of fBM cDC, along with enhancing the concomitant
232 functional maturation of these cDC as demonstrated by upregulated I-A/I-E (MHC Class II)
233 expression. This BM population is the source of the precursors which subsequently seed the
234 airway mucosal DC network that progressively develops between birth and weaning[3, 4]. It is
235 noteworthy that the cDC which initially seed this network postnatally are MHC-II$^{low}$ (reflecting
236 their functionally immature status) relative to the high-level expression seen at later ages[3],
237 and the findings above in fetal cDC from the treated group may collectively explain the
238 accelerated postnatal establishment and the enhanced functional maturation of this network
239 observed in their offspring[15]. This DC network plays an essential "gatekeeper" role in immune

240 surveillance of airway surfaces, and hence in protection against both allergic and infectious
241 diseases in the respiratory tract[38, 39], and its relative paucity and reduced functionality during
242 infancy may be an important contributor to increased susceptibility to these diseases during
243 this life phase.
244
245 Earlier studies from our group also identified unique features of the population dynamics of
246 this lung cDC network which distinguishes it from comparable populations in other tissues,
247 notably the exceptionally rapid baseline turnover rate of individual cells within the network,
248 ~85% of which are replaced every 24-36 hours[40], with emigration to draining lymph nodes
249 (bearing samples of locally acquired antigens) balanced by recruitment of replacements from
250 BM. Moreover, once development of functional competence is complete[4], this network
251 develops capability for rapid expansion to up to 5-fold baseline density in the face of acute
252 challenge with airborne pro-inflammatory irritant, allergenic or microbial stimuli[41], the latter
253 response exhibiting kinetics that rival neutrophils[42, 43]. These unique population dynamics
254 suggests that even at baseline, mechanisms that promote lung cDC survival are likely to play
255 a crucial role in the capacity of the network to perform its immune surveillance functions
256 which require onward migration to downstream lymph nodes and subsequent interaction
257 with T-cells as opposed to antigen presentation *in situ*[38]; moreover during prolonged/severe
258 events exemplified by severe viral infections, the added effects of cDC injury resulting from
259 inflammation-associated ER stress[44] would place further pressure on survival times.
260
261 In this regard, our transcriptomic analyses of fBM from offspring of OM-85-treated mothers
262 also identified upregulated expression of XBP1, ATF6$\beta$ and ERN1 (encoding IRE1$\alpha$), key
263 components of the XBP1-ERN1 signalling axis and critical regulators of the UPR pathway[45]

264 which mitigates the effects of ER stress, and moreover we localised upregulated production
265 of active XBP1s protein to cDC precursors. Taken together with recent findings on the role for
266 IRE1$\alpha$-XBP1 signalling and the downstream transcription factor XBP1s in DC development and
267 function[22, 23], these results suggest a central role for the XBP1-ERN1 signalling axis in this OM-
268 85-mediated immune training process.
269
270 In further support of this suggestion, other studies demonstrate a significant reduction in
271 CD11c$^{+}$ cells (mirroring that of our pre-cDC phenotype) within XBP1$^{-/-}$ BM cultures, whilst
272 forced overexpression of XBP1s in XBP1$^{-/-}$ DC precursors conversely rescues and subsequently
273 drives expansion of the DC pool *in vitro*[22]. It is also pertinent to note that others have reported
274 that the cDC population in the lung mucosa is differentially reliant upon XBP1 expression for
275 survival at baseline relative to cDC from other tissue sites[44], which may be a direct reflection
276 of the uniquely high turnover rates of cDC within the airway mucosal microenvironment[40].
277
278 Collectively, the data presented here indicate that OM-85 likely operates as an immune
279 training agent, employing cellular and immunometabolic mechanisms previously reported in
280 independent model systems[10, 11, 46], with the additional capacity to act transplacentally via the
281 fBM. Furthermore, we go beyond the currently known features of innate immune training to
282 describe involvement of the XBP1-ERN1 signalling axis. Moreover, classical $\beta$-glucan- and
283 BCG-mediated immune training has traditionally focused on prototypic innate effector cell
284 populations (monocytes/macrophages/natural killer cells) resulting in enhanced resistance to
285 bystander pathogens via the upregulation of pro-inflammatory responses exemplified by
286 tumour necrosis factor-$\alpha$ (TNF-$\alpha$), interferon-$\gamma$ (IFN-$\gamma$), IL-6 and IL-1$\beta$ production[47-49] and
287 emergency granulopoiesis-mediated neutrophilic influx[46]. However, studies are now

288 beginning to recognise that immune training can also occur in DC populations, resulting *inter*
289 *alia* in epigenetic reprograming of pro-inflammatory cytokine responses[50]. We have recently
290 extended these observations to include OM-85-mediated training effects on key
291 immunoregulatory functions in both pregnant mice and their offspring, including effects on
292 both cDC and pDC populations and downstream T-regulatory cells, which are collectively
293 associated with enhanced resistance of both mothers and offspring to the pro-inflammatory
294 effects of bacterial, viral and allergenic stimulation[15, 51]. Of note, similar transplacental
295 immune training-like effects targeting immunoregulatory mechanisms in offspring have been
296 reported in relation to pregnant maternal exposure to extracts from *Acinetobacter lwoffii*[52]
297 and *Helicobacter pylori*[53], suggesting that the phenomenon reported here may be
298 generalisable, and may point towards a novel approach to mitigation of disease risk in the age
299 group that is in greatest need of protection.
300
301 **Methods**
302 ***Animals***
303 Specific pathogen-free BALB/c mice were purchased from the Animal Resource Centre
304 (Murdoch, Western Australia, Australia). All mice were housed under specific pathogen-free
305 conditions at the Telethon Kids Institute Bioresources Centre.
306
307 ***Time-mated pregnancies***
308 Female BALB/c mice 8-12 weeks of age were time-mated with male BALB/c studs 8-26 weeks
309 of age. Male studs were housed individually with 1-2 females overnight. The detection of a
310 vaginal plug the following morning was designated gestation day (GD) 0.5.
311

312 ***Maternal OM-85 treatment***

313 OM-85 (OM Pharma) is an endotoxin-low lyophilised extract containing a cocktail of TLR
314 ligands derived from 8 major respiratory tract bacterial pathogens (*Haemophilus influenzae,*
315 *Streptococcus pneumoniae, Streptococcus pyogenes, Streptococcus viridians, Klebsiella*
316 *pneumoniae, Klebsiella ozaenae, Staphylococcus aureus* and *Neisseria catarrhalis*)[54, 55]. Based
317 on previously optimised dosing concentrations[51, 56], time-mated pregnant BALB/c mice
318 selected at random received daily oral feeding of lyophilised OM-85 reconstituted in
319 phosphate-buffered saline (PBS) to a concentration of 400mg/kg body weight for the second
320 half of gestation (GD9.5 – 17.5). Control pregnant mice were left untreated for the duration
321 of the study. All maternal treatment was performed with a single batch of OM-85 (batch
322 1812162).

323

324 ***Tissue collection***

325 Pregnant BALB/c mice were sacrificed 24 hours after the final OM-85 dose at GD18.5. Both
326 horns of the uterus were removed and fetuses sacrificed by decapitation. Fetal hind legs
327 (cleaned of excess tissue) were removed. Fetal hind leg samples for flow cytometry were
328 collected into cold PBS + 0.1% bovine serum albumin (BSA) and stored on ice. Fetal hind leg
329 samples for transcriptomic analysis were collected into RNAlater® stabilisation solution
330 (Ambion). Samples collected into RNAlater® were stored overnight at 4°C, then transferred
331 to 1.5ml Eppendorf tubes (Eppendorf) and frozen at -80°C for future transcriptome profiling.
332 Dead fetuses were excluded from the study.

333

334

335

336 ***Single-cell suspension preparation***

337 Fetal hind legs were prepared by mincing with a scalpel followed by enzymatic digestion, as
338 previously detailed[15]. Briefly, minced tissue was resuspended in 10ml GKN + 10% fetal calf
339 serum (FCS; Serana) with collagenase IV (Worthington Biochemical Corp.) and DNase (Sigma-
340 Aldrich) at 37°C under gentle agitation for 60 minutes. Digested cells were filtered through
341 sterile cotton wool columns, centrifuged and resuspended in cold PBS for total cell counts.

342

343 ***Flow cytometry***

344 Fetal bone marrow single-cell suspensions were used for all immunostaining. Panels of
345 monoclonal antibodies were developed to enable phenotypic characterisation of committed
346 myeloid cells: CD3-FITC (BD Bioscience; clone 17A2), CD11b-BV510 (BD Bioscience; clone
347 M1/70), CD11c-BV711 (BD Bioscience; clone HL3), CD19-APC-H7 (BD Bioscience; clone 1D3),
348 Gr-1-Biotin (BD Bioscience; clone RB6-6B2), CD45R/B220-PerCP-Cy5.5 (BD Bioscience; clone
349 RA3-6B2) NKp46-PE-Cy7 (BioLegend; clone 29A1.4), SIRP-α-APC (BioLegend; clone P84), I-A/I-
350 E-BV421 (BioLegend; clone M5/114.15.2), F4/80-BV785 (BioLegend; clone BM8), Viability-
351 AF700 (BD Bioscience), Streptavidin-BV605 (BD Bioscience); hematopoietic stem and
352 progenitor cells: CD2-Biotin (BD Bioscience; clone RM2-5), CD3-Biotin (BD Bioscience; clone
353 145-2C11), CD4-Biotin (BD Bioscience; clone GK1.5), CD5-Biotin (BD Bioscience; clone 53-7.3),
354 CD8α-Biotin (BD Bioscience; clone 53-6.7), CD19-Biotin (BD Bioscience; clone 1D3),
355 CD45R/B220-Biotin (BD Bioscience; RA3-6B2), Gr-1-Biotin (BD Bioscience; clone RB6-6B2),
356 Ter119-Biotin (BD Bioscience; clone TER-119), CD16/32-PerCP-Cy5.5 (BD Bioscience; clone
357 2.4G2), CD34-FITC (BD Bioscience; clone RAM34), IL-7Rα-PE-Cy7 (BD Bioscience; clone
358 SB/199), Flt-3-PE (BD Bioscience; clone A2F10.1), c-Kit-APC-Cy7 (BD Bioscience; clone 2B8),
359 Sca-1-BV510 (BD Bioscience; clone D7), CX3CR1-APC (BioLegend; clone SA011F11), NKG2D-

360 BV711 (BD Bioscience; CX5), Viability-AF700 (BD Bioscience), Streptavidin-BV605 (BD
361 Bioscience) and XBP1s-expressing bone marrow cells: CD3-FITC (BD Bioscience; clone 17A2),
362 CD11b-BV510 (BD Bioscience; clone M1/70), CD11c-AF700 (BD Bioscience; clone HL3), CD19-
363 APC-H7 (BD Bioscience; clone 1D3), I-A/I-E-AF647 (BD Bioscience; clone M5/114.15.2),
364 CD45R/B220-PE-CF594 (BD Bioscience; RA3-6B2), Gr-1-Biotin (BD Bioscience; clone RB6-6B2),
365 NKp46-PE-Cy7 (BioLegend; clone 29A1.4), F4/80-BV785 (BioLegend; clone BM8), XBP1s-
366 BV421 (BD Bioscience; clone Q3-695), Streptavidin-BV605 (BD Bioscience). Intracellular
367 staining for XBP1s was performed using an intracellular staining buffer kit (eBioscience). Data
368 acquisition was performed on a 4-laser LSR Fortessa (BD Bioscience). All samples were kept
369 as individuals and not pooled. Immune cell phenotypic characterisation was performed using
370 FlowJo software (version 10.1, Tree Star). Fluorescence minus one staining controls were used
371 for all panels.
372
373 ***Flow cytometric statistical analyses***
374 Statistical analysis and graphing was performed using GraphPad Prism (GraphPad software;
375 version 7.0a). Statistical significance of $p<0.05$ was considered significant. Unpaired, two-
376 tailed Student's *t*-test or Mann Whitney *U* test were used based on distribution of the data as
377 determined by D'Agostino-Pearson omnibus normality test. Part of the cDC flow cytometry
378 data presented in Figure 1 and MDP data presented in Figure 2 has been published in a
379 forerunner manuscript[15].
380
381 ***Transcriptome profiling (RNA-Seq)***
382 *Tissue preparation, RNA extraction and transcriptome profiling.* Fetal bone marrow samples
383 were homogenised using a rotor-star homogeniser (Qiagen) and total RNA extracted via

384 TRIzol (Ambion), followed by clean-up using RNeasy MinElute (Qiagen). RNA integrity was
385 determined using an Agilent 2100 Bioanalyzer (Agilent Technologies; RIN: $10 \pm 0$ (mean $\pm$ SD)).
386 1μg total RNA ($n$ = 32) was shipped on dry ice to the Australia Genome Research Facility
387 (AGRF) for library preparation (TruSeq Stranded mRNA Library Prep Kit, Illumina) and
388 sequencing (Illumina HiSeq2500, 50-bp singe-end reads, v4 chemistry). The raw sequencing
389 data are available from GEO (accession; GSE140143).
390
391 ***RNA-Seq data analysis***
392 *Pre-processing and exploratory data analysis:* RNA-Seq data was analysed in the R
393 environment for statistical computing. Sequencing data quality control (QC) was performed
394 with the Bioconductor package Rqc[57]. Sequencing reads were aligned to the reference murine
395 genome (mm10) using Subread and summarised at the gene level using featureCounts[58].
396 Genes with <500 total counts across the data were removed from the analysis. Sample QC
397 was performed by analysing the distribution of the raw read counts to check for sample
398 outliers using boxplots, relative log-transformed expression (RLE) plots and principal
399 component analysis (PCA), before and after global-scale median normalisation. *Differential*
400 *expression analysis:* Differentially expressed genes (DEG) were identified employing the
401 *DESeq2* package[59]. *DESeq2* utilises a negative binomial distribution model, with a False
402 Discovery Rate adjusted *P*-value for multiple comparisons. Genes were deemed significant
403 with an adjusted *P*-value < 0.1. *Pathways analysis:* Pathways enrichment analysis was
404 performed using the InnateDB database[16] with Benjamini & Hochberg adjusted *P*-value $\leq 0.05$
405 deemed significant. *Upstream regulator analysis:* Ingenuity Systems Upstream Regulator
406 Analysis[60] was employed to identify putative molecular drives of the DEG patterns.
407 Significance was determined by activation Z-score $\geq 2$ and *P*-value of overlap $\leq 0.05$.

408 ***Study approval***

409 All animal experiments were formally approved by the Telethon Kids Institute Animal Ethics
410 Committee, operating under the guidelines developed by the National Health and Medical
411 Research Council of Australia for the care and use of animals in scientific research.

412

413 **Acknowledgements**

414 The authors wish to acknowledge the animal technicians at the Telethon Kids Institute
415 Bioresources Centre. This study was funded by the National Health and Medical Research
416 Council of Australia. OM Pharma provided the OM-85 at no cost.

417

418 **Author contributions**

419 KTM, PGH and DHS designed the study. KTM, MB, NMS and JFLJ performed the experiments.
420 KTM, ACJ, MB and DHS analysed the data. PAS and AB contributed to the project design and
421 discussions on data interpretation. KTM, PAS, PGH and DHS wrote the manuscript. All authors
422 reviewed the final version of the manuscript.

423

424

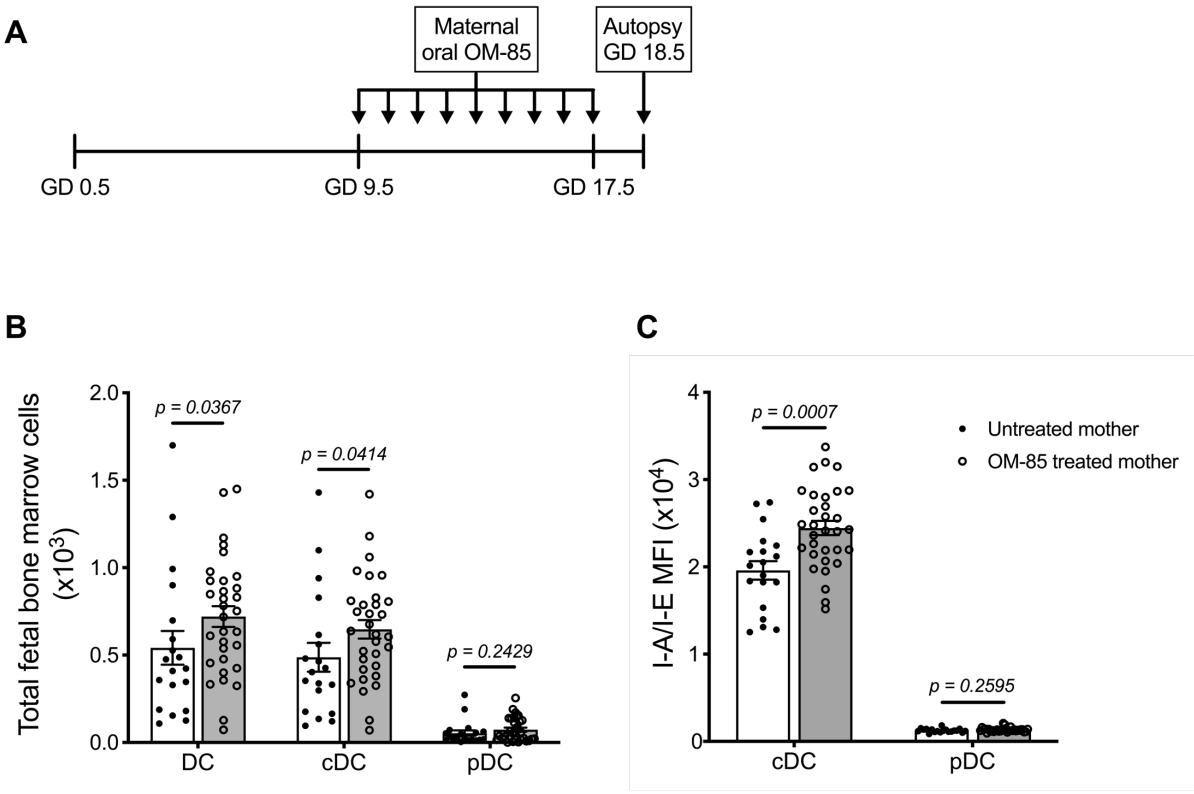


425

426 **Figure 1. Maternal OM-85 treatment during pregnancy selectively modulates the fetal bone**
427 **marrow conventional DC subset. (A)** Kinetics of maternal OM-85 treatment beginning at
428 gestation day (GD) 9.5 with daily oral treatment until GD 17.5 and autopsy 24 hours post final
429 treatment at GD 18.5. **(B)** Absolute numbers of dendritic cells (DC), $CD11b^{+}B220^{-}CD11c^{+}Gr\text{-}1^{-}$
430 $SIRP\text{-}\alpha^{+}I\text{-}A/I\text{-}E^{+}$ conventional dendritic cells (cDC) and $CD11b^{-}B220^{+}CD11c^{+}Gr\text{-}1^{+}I\text{-}A/I\text{-}E^{+}$
431 plasmacytoid dendritic cells (pDC) in BM of fetuses from OM-85-treated and untreated
432 mothers. **(C)** Mean fluorescence intensity (MFI) of I-A/I-E expression on cDCs and pDCs in fBM.
433 Data are presented from individual animals comparing fetuses from OM-85-treated and
434 untreated mothers and displayed as bar graphs showing mean ± SEM of *n* = 8 independent
435 experiments. Statistical significance was determined using Mann-Whitney *U* test (B) or
436 Student's *t* test (C) based on distribution of the data as determined by D'Agostino-Pearson
437 omnibus normality test.

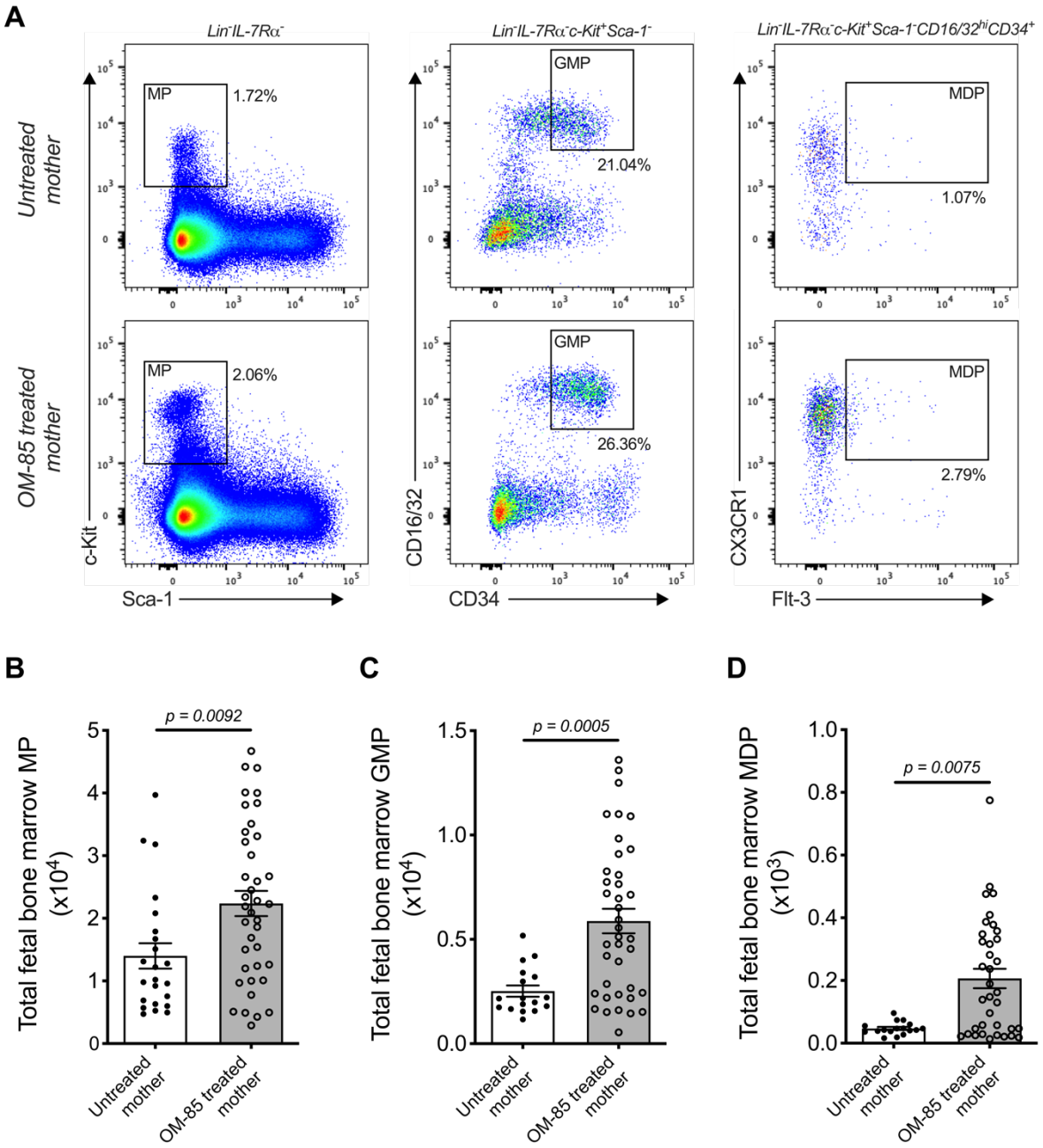


**Figure 2. Treatment of mothers with OM-85 during pregnancy boosts myeloid progenitor subsets within fetal bone marrow. (A)** Representative flow cytometry plots for the identification of Lin$^-$IL-7Rα$^-$c-Kit$^+$Sca-1$^-$ myeloid progenitors (MP), Lin$^-$IL-7Rα$^-$c-Kit$^+$Sca-1$^-$ CD16/32$^{hi}$CD34$^+$ granulocyte-macrophage progenitors (GMP) and Lin$^-$IL-7Rα$^-$c-Kit$^+$Sca-1$^-$ CD16/32$^{hi}$CD34$^+$CX3CR1$^+$Flt-3$^+$ macrophage-dendritic cell progenitors (MDP) within fBM. Absolute numbers of **(B)** MP, **(C)** GMP and **(D)** MDP in BM of fetuses from OM-85-treated and

445 untreated mothers. Data are presented from individual animals comparing fetuses from OM-
446 85-treated and untreated mothers and displayed as bar graphs showing mean ± SEM of $n$ = 8
447 independent experiments. Statistical significance was determined using Student's $t$ test (C) or
448 Mann-Whitney $U$ test (B, D) based on distribution of the data as determined by D'Agostino-
449 Pearson omnibus normality test.

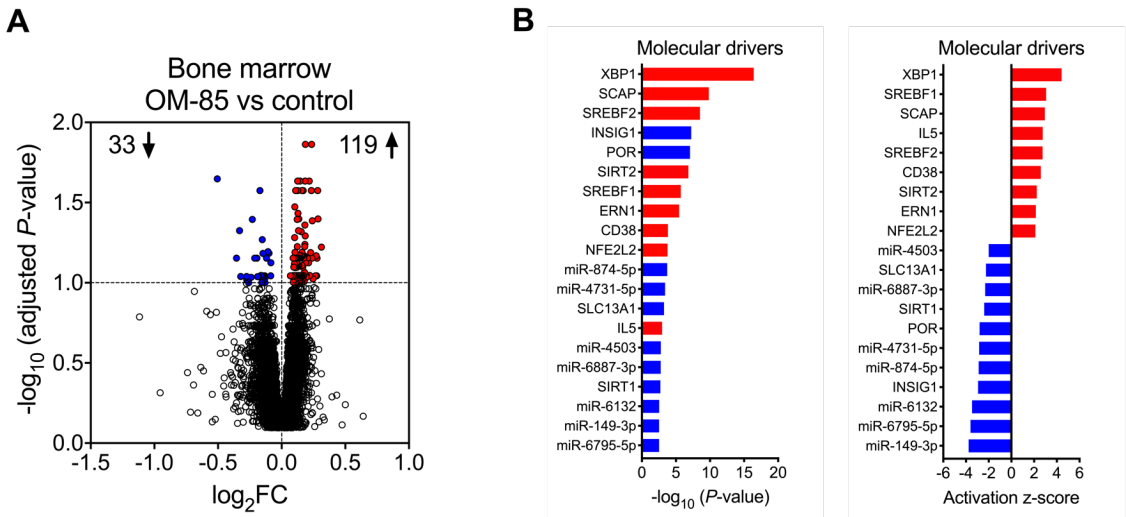


**Figure 3. Maternal OM-85-induced changes in fetal bone marrow gene expression profiles.** **(A)** Differentially expressed genes (DEG) within fBM comparing offspring from OM-85-treated and untreated mothers. DEG are summarised as a volcano plot showing data along axes of statistical significance ($-\log_{10}$ adjusted *P*-value) and differential expression magnitude ($\log_2$ fold change) for $n$ = 16 individual animals per group collected from $n$ = 7 independent experiments. Dashed horizontal lines indicate a False Discovery Rate (FDR) adjusted *P*-value < 0.1. Genes shown in red were upregulated and those shown in blue were downregulated. **(B)** activated (red) and inhibited (blue) molecular drivers of the differential expression patterns were identified using Upstream Regulator Analysis.

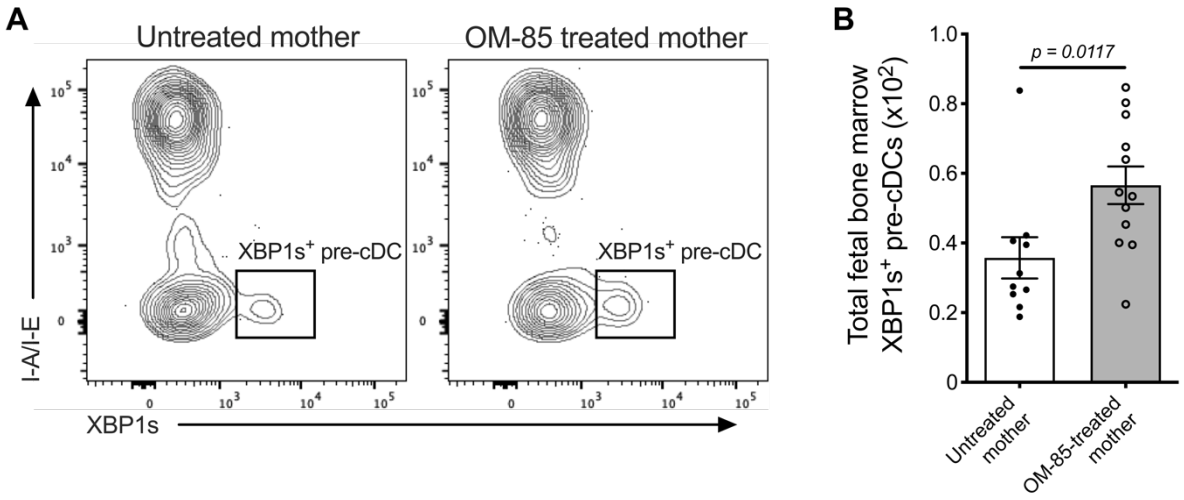


462

463 **Figure 4. XBP1s expression in pre-cDCs within fetal bone marrow. (A)** Representative flow

464 cytometry plots demonstrating intracellular XBP1s expression in $CD11b^{+}B220^{-}CD11c^{+}Gr\text{-}1^{-}I\text{-}$

465 $A/I\text{-}E^{-}XBP1s^{+}$ pre-conventional dendritic cells (pre-cDCs) within fBM. **(B)** Absolute numbers of

466 $XBP1s^{+}$ pre-cDCs in BM of fetuses from OM-85-treated and untreated mothers. Data are

467 presented from individual animals comparing fetuses from OM-85-treated and untreated

468 mothers and displayed as bar graphs showing mean $\pm$ SEM of $n$ = 4 independent experiments.

469 Statistical significance was determined using Mann-Whitney *U* test.

470

471

472 **References**


473 1. Levy O. Innate immunity of the newborn: basic mechanisms and clinical correlates.
474 Nat Rev Immunol. 2007;7(5):379-90.

475 2. Adkins B, Leclerc C, Marshall-Clarke S. Neonatal adaptive immunity comes of age. Nat
476 Rev Immunol. 2004;4(7):553-64.

477 3. Nelson DJ, McMenamin C, McWilliam AS, Brenan M, Holt PG. Development of the
478 airway intraepithelial dendritic cell network in the rat from class II major
479 histocompatibility (Ia)-negative precursors: differential regulation of Ia expression at
480 different levels of the respiratory tract. J Exp Med. 1994;179(1):203-12.

481 4. Nelson DJ, Holt PG. Defective regional immunity in the respiratory tract of neonates is
482 attributable to hyporesponsiveness of local dendritic cells to activation signals. J
483 Immunol. 1995;155(7):3517-24.

484 5. Gollwitzer ES, Marsland BJ. Impact of Early-Life Exposures on Immune Maturation and
485 Susceptibility to Disease. Trends Immunol. 2015;36(11):684-96.

486 6. Apostol AC, Jensen KDC, Beaudin AE. Training the Fetal Immune System Through
487 Maternal Inflammation-A Layered Hygiene Hypothesis. Front Immunol. 2020;11:123-
488 36.

489 7. von Mutius E, Vercelli D. Farm living: effects on childhood asthma and allergy. Nat Rev
490 Immunol. 2010;10(12):861-8.

491 8. Ober C, Sperling AI, von Mutius E, Vercelli D. Immune development and environment:
492 lessons from Amish and Hutterite children. Curr Opin Immunol. 2017;48:51-60.

493 9. Kleinnijenhuis J, et al. Long-lasting effects of BCG vaccination on both heterologous
494 Th1/Th17 responses and innate trained immunity. J Innate Immun. 2014;6(2):152-8.

495 10. Mitroulis I, et al. Modulation of Myelopoiesis Progenitors Is an Integral Component of
496 Trained Immunity. Cell. 2018;172(1-2):147-61.
497 11. Kaufmann E, et al. BCG Educates Hematopoietic Stem Cells to Generate Protective
498 Innate Immunity against Tuberculosis. Cell. 2018;172(1):176-90.e19.
499 12. Netea MG, et al. Defining trained immunity and its role in health and disease. Nat Rev
500 Immunol. 2020.
501 13. Mulder WJM, Ochando J, Joosten LAB, Fayad ZA, Netea MG. Therapeutic targeting of
502 trained immunity. Nat Rev Drug Discov. 2019;18(7):553-66.
503 14. Holt PG, Strickland DH, Custovic A. Targeting maternal immune function during
504 pregnancy for asthma prevention in offspring: harnessing the “farm effect”? J Allergy
505 Clin Immunol. 2020;*In-press*.
506 15. Mincham KT, et al. Transplacental immune modulation with a bacterial-derived agent
507 protects against allergic airway inflammation. J Clin Invest. 2018;128(11):4856-69.
508 16. Breuer K, et al. InnateDB: systems biology of innate immunity and beyond-recent
509 updates and continuing curation. Nucleic Acids Res. 2013;41(Database issue):D1228-
510 33.
511 17. Iwakoshi NN, et al. Plasma cell differentiation and the unfolded protein response
512 intersect at the transcription factor XBP-1. Nat Immunol. 2003;4(4):321-9.
513 18. Reimold AM, et al. Plasma cell differentiation requires the transcription factor XBP-1.
514 Nature. 2001;412(6844):300-7.
515 19. Bettigole SE, et al. The transcription factor XBP1 is selectively required for eosinophil
516 differentiation. Nat Immunol. 2015;16(8):829-37.
517 20. Dong H, et al. The IRE1 endoplasmic reticulum stress sensor activates natural killer cell
518 immunity in part by regulating c-Myc. Nat Immunol. 2019;20(7):865-78.

519 21. Pramanik J, et al. Genome-wide analyses reveal the IRE1a-XBP1 pathway promotes T
520 helper cell differentiation by resolving secretory stress and accelerating proliferation.
521 Genome Med. 2018;10(1):76.
522 22. Iwakoshi NN, Pypaert M, Glimcher LH. The transcription factor XBP-1 is essential for
523 the development and survival of dendritic cells. J Exp Med. 2007;204(10):2267-75.
524 23. Osorio F, et al. The unfolded-protein-response sensor IRE-1alpha regulates the
525 function of CD8alpha+ dendritic cells. Nat Immunol. 2014;15(3):248-57.
526 24. Yoshida H, et al. Endoplasmic reticulum stress-induced formation of transcription
527 factor complex ERSF including NF-Y (CBF) and activating transcription factors 6alpha
528 and 6beta that activates the mammalian unfolded protein response. Mol Cell Biol.
529 2001;21(4):1239-48.
530 25. Yoshida H, Matsui T, Yamamoto A, Okada T, Mori K. XBP1 mRNA is induced by ATF6
531 and spliced by IRE1 in response to ER stress to produce a highly active transcription
532 factor. Cell. 2001;107(7):881-91.
533 26. Xia B, et al. Upregulation of miR-874-3p and miR-874-5p inhibits epithelial ovarian
534 cancer malignancy via SIK2. J Biochem Mol Toxicol. 2018;32(8):e22168.
535 27. Stark MS, et al. The "melanoma-enriched" microRNA miR-4731-5p acts as a tumour
536 suppressor. Oncotarget. 2016;7(31):49677-87.
537 28. Yang D, Du G, Xu A, Xi X, Li D. Expression of miR-149-3p inhibits proliferation,
538 migration, and invasion of bladder cancer by targeting S100A4. Am J Cancer Res.
539 2017;7(11):2209-19.
540 29. Shen W, et al. Repression of Toll-like receptor-4 by microRNA-149-3p is associated
541 with smoking-related COPD. Int J Chron Obstruct Pulmon Dis. 2017;12:705-15.

542 30. Kirchner B, Pfaffl MW, Dumpler J, von Mutius E, Ege MJ. microRNA in native and
543 processed cow's milk and its implication for the farm milk effect on asthma. J Allergy
544 Clin Immunol. 2016;137(6):1893-5.e13.
545 31. Todd DJ, et al. XBP1 governs late events in plasma cell differentiation and is not
546 required for antigen-specific memory B cell development. J Exp Med.
547 2009;206(10):2151-9.
548 32. Goldstein JL, DeBose-Boyd RA, Brown MS. Protein sensors for membrane sterols. Cell.
549 2006;124(1):35-46.
550 33. Tolani S, et al. Hypercholesterolemia and reduced HDL-C promote hematopoietic stem
551 cell proliferation and monocytosis: studies in mice and FH children. Atherosclerosis.
552 2013;229(1):79-85.
553 34. Yvan-Charvet L, et al. ATP-binding cassette transporters and HDL suppress
554 hematopoietic stem cell proliferation. Science (New York, NY). 2010;328(5986):1689-
555 93.
556 35. Murphy AJ, et al. ApoE regulates hematopoietic stem cell proliferation, monocytosis,
557 and monocyte accumulation in atherosclerotic lesions in mice. J Clin Invest.
558 2011;121(10):4138-49.
559 36. Morgan PK, Fang L, Lancaster GI, Murphy AJ. Hematopoiesis is regulated by
560 cholesterol efflux pathways and lipid rafts: connections with cardiovascular diseases.
561 J Lipid Res. 2020;61(5):667-75.
562 37. Yang T, et al. Crucial step in cholesterol homeostasis: sterols promote binding of SCAP
563 to INSIG-1, a membrane protein that facilitates retention of SREBPs in ER. Cell.
564 2002;110(4):489-500.

565 38. Holt PG, Strickland DH, Wikstrom ME, Jahnsen FL. Regulation of immunological
566 homeostasis in the respiratory tract. Nat Rev Immunol. 2008;8(2):142-52.
567 39. Lambrecht BN, Hammad H. Lung dendritic cells in respiratory viral infection and
568 asthma: from protection to immunopathology. Annu Rev Immunol. 2012;30:243-70.
569 40. Holt PG, Haining S, Nelson DJ, Sedgwick JD. Origin and steady-state turnover of class
570 II MHC-bearing dendritic cells in the epithelium of the conducting airways. J Immunol.
571 1994;153(1):256-61.
572 41. McWilliam AS, et al. Dendritic Cells Are Recruited into the Airway Epithelium during
573 the Inflammatory Response to a Broad Spectrum of Stimuli. J Exp Med.
574 1996;184(6):2429-32.
575 42. Jahnsen FL, et al. Accelerated antigen sampling and transport by airway mucosal
576 dendritic cells following inhalation of a bacterial stimulus. J Immunol.
577 2006;177(9):5861-7.
578 43. McWilliam AS, Nelson D, Thomas JA, Holt PG. Rapid dendritic cell recruitment is a
579 hallmark of the acute inflammatory response at mucosal surfaces. J Exp Med.
580 1994;179(4):1331-6.
581 44. Tavernier SJ, et al. Regulated IRE1-dependent mRNA decay sets the threshold for
582 dendritic cell survival. Nat Cell Biol. 2017;19(6):698-710.
583 45. Grootjans J, Kaser A, Kaufman RJ, Blumberg RS. The unfolded protein response in
584 immunity and inflammation. Nat Rev Immunol. 2016;16(8):469-84.
585 46. Brook B, et al. BCG vaccination–induced emergency granulopoiesis provides rapid
586 protection from neonatal sepsis. Sci Transl Med. 2020;12(542):eaax4517.
587 47. Quintin J, et al. Candida albicans infection affords protection against reinfection via
588 functional reprogramming of monocytes. Cell Host Microbe. 2012;12(2):223-32.

589 48. Kleinnijenhuis J, et al. Bacille Calmette-Guerin induces NOD2-dependent nonspecific
590 protection from reinfection via epigenetic reprogramming of monocytes. Proc Natl
591 Acad Sci U S A. 2012;109(43):17537-42.
592 49. Sun JC, Beilke JN, Lanier LL. Adaptive Immune Features of Natural Killer Cells. Nature.
593 2009;457(7229):557-61.
594 50. Hole CR, et al. Induction of memory-like dendritic cell responses in vivo. Nat Commun.
595 2019;10(1):2955.
596 51. Scott NM, et al. Protection against maternal infection-associated fetal growth
597 restriction: proof-of-concept with a microbial-derived immunomodulator. Mucosal
598 Immunol. 2017;10(3):789-801.
599 52. Conrad ML, et al. Maternal TLR signaling is required for prenatal asthma protection by
600 the nonpathogenic microbe Acinetobacter lwoffii F78. J Exp Med. 2009;206(13):2869-
601 77.
602 53. Kyburz A, et al. Transmaternal Helicobacter pylori exposure reduces allergic airway
603 inflammation in offspring through regulatory T cells. J Allergy Clin Immunol.
604 2019;143(4):1496-512.e11.
605 54. Razi CH, et al. The immunostimulant OM-85 BV prevents wheezing attacks in
606 preschool children. J Allergy Clin Immunol. 2010;126(4):763-9.
607 55. Rozy A, Chorostowska-Wynimko J. Bacterial immunostimulants--mechanism of action
608 and clinical application in respiratory diseases. Pneumonol Alergol Pol.
609 2008;76(5):353-9.
610 56. Strickland DH, et al. Boosting airway T-regulatory cells by gastrointestinal stimulation
611 as a strategy for asthma control. Mucosal Immunol. 2011;4(1):43-52.

612 57. de Souza W, Carvalho BdS, Lopes-Cendes I. Rqc: A Bioconductor Package for Quality
613 Control of High-Throughput Sequencing Data. Journal of Statistical Software, Code
614 Snippets. 2018;87(2):1-14.
615 58. Liao Y, Smyth GK, Shi W. The Subread aligner: fast, accurate and scalable read mapping
616 by seed-and-vote. Nucleic Acids Res. 2013;41(10):e108.
617 59. Love MI, Huber W, Anders S. Moderated estimation of fold change and dispersion for
618 RNA-seq data with DESeq2. Genome Biol. 2014;15(12):550.
619 60. Krämer A, Green J, Pollard J, Jr., Tugendreich S. Causal analysis approaches in Ingenuity
620 Pathway Analysis. Bioinformatics. 2014;30(4):523-30.
621